

Chapter 2

Global Monsoon in a Changing Climate

Pang-Chi Hsu

Abstract Monsoons, the most energetic tropical climate system, exert a great social and economic impact upon billions of people around the world. This chapter reviews recent progress in our understanding of the global monsoon (GM) system and its associated precipitation changes in the present and future warming climates. The GM can be viewed as an integrated system of all regional monsoons over the globe that are driven by solar forcing and bounded by the planetary-scale overturning circulation. The GM precipitation (GMP), defined as the total summer monsoon precipitation amount within the GM area (GMA), experienced multi-decadal variability in the twentieth century. The observed GMP over land shows a slightly increasing trend from 1900 throughout the 1940s, and then a downward trend from the 1950s until the end of the 1970s; there was no clear trend after 1980. The GMP over the ocean has had more uncertainty over the past three decades, and trends are inconsistent among different global rainfall datasets. In the twenty-first century, the GMP is expected to increase robustly, based on the projections by the state-of-the-art coupled models that participated in Phases 3 and 5 of the Coupled Model Intercomparison Project (CMIP3 and CMIP5). The change in GMP under global warming is primarily due to changes to the hydrological cycle induced by warmer temperatures. The increase in water vapor contributes positively to moisture convergence and surface evaporation over the GMA, but is partly offset by the weakening of the monsoon circulation.

Keywords Global monsoon · Monsoon precipitation variability · Global warming · CMIP3 · CMIP5

P.-C. Hsu (✉)

International Laboratory on Climate and Environment Change and College of Atmospheric Science, Nanjing University of Information Science and Technology, Nanjing, China
e-mail: pangchi@hawaii.edu

P.-C. Hsu

International Pacific Research Center, University of Hawaii, Honolulu, HI, USA

2.1 Introduction

“Monsoon” is conventionally defined as the seasonal reversal in lower-tropospheric winds (Ramage 1971), and its associated precipitation is characterized by a contrast between wet summers and dry winters (Webster 1987). The contrast is induced by the annual cycle of solar heating and seasonal changes in large-scale continent-ocean thermal contrast. Monsoons occur around the globe: in Asia, Australia, Africa, and throughout the Americas (Webster et al. 1998). From a regional perspective, an individual monsoon system evolves according to the local land-sea configuration, orography, and feedback with the distinct elements of the climate system. The features and variations of each regional monsoon have been extensively studied over the past three decades (e.g., Davidson et al. 1983; McBride 1987; Tao and Chen 1987; Webster 1987; Ding 1994; Higgins et al. 1997; Webster et al. 1998; Sultan and Janicot 2003; Goswami 2005; Vera et al. 2006).

More recently, an emerging concept of the global monsoon (GM) has been proposed to describe the combined variability of monsoon systems around the world. Considering that all regional monsoons are associated with the annual cycle of solar heating and that the global-scale circulation is necessitated by mass conservation, Trenberth et al. (2000) depicted the GM system as a persistent global-scale overturning of the tropical atmosphere that varies with seasons. In a dynamic sense, the rainfall distributions reflect the tropospheric heat sources that drive the circulation in the tropics; thus, the planetary-scale overturning circulation is closely associated with the seasonal variation of precipitation. Wang and Ding (2008) documented that in the climatological context, the GM system is the dominant mode of annual precipitation and 850 hPa winds in the tropics. Applying a multi-variable empirical orthogonal function (EOF) analysis to climatological monthly precipitation and low-level wind fields, two leading modes—accounting for 84 % of the annual variance—were obtained. The first mode, called the solstitial mode, represents the atmospheric response to the meridional differential of annual solar forcing. The second mode, the equinoctial asymmetry mode, reflects the asymmetric patterns between spring and autumn. Both modes characterize the seasonality of tropical climate (Wang and Ding 2008).

In short, the GM is a response of the coupled climate system to the annual cycle of solar forcing. From this global perspective, the precipitation over each monsoon region combines to form the GM system, which is associated with a planetary-scale overturning circulation throughout the tropics (Trenberth et al. 2000, 2006).

2.2 Delineations of Global Monsoon Precipitation, Area, and Intensity

The monsoon climate features the seasonal variations in both wind and precipitation. Earlier studies used the reversal in wind direction and speed to identify a monsoon domain (Ramage 1971). Such monsoon domains are found mainly over

the Eastern Hemisphere because the seasonal wind reversal is less significant over the Americas. Besides the wind field, precipitation is another fundamental variable used to delineate the monsoon climate. Monsoon precipitation is characterized by a concentration of yearly rainfall in the local summer and a dry period in the local winter (Webster 1987). Using a simple parameter based on precipitation, Wang and Ding (2006) defined the global monsoon area (GMA) as the regions in which the annual range (AR—the local summer-minus-winter rainfall) of rainfall exceeds 180 mm and the summer-to-annual rainfall ratio is greater than 35 %. In the Northern Hemisphere (NH), the summer is defined as June to August (JJA) and the winter is defined as December to February (DJF). In the Southern Hemisphere (SH), the definitions are reversed. Figure 2.1 shows the derived GMA based on the climatological monthly rainfall averaged from the Global Precipitation Climatology Project (GPCP; Adler et al. 2003) and the CPC Merged Analysis of Precipitation (CMAP; Xie and Arkin 1997) datasets. The known monsoon systems around the world, including the Asian, Australian, northern and southern African, and North and South American Monsoons, are well identified.

Following the approach of Wang and Ding (2006), other studies modified the lengths of summer and winter seasons and the criteria of rainfall indices. For example, Liu et al. (2009) used a longer length of local summer (May to September (MJJAS) for the NH) and winter (November to March (NDJFM) for the SH) months. The two criteria for GMA were modified as the AR (MJJAS and NDJFM difference) exceeding 2 mm day^{-1} and the ratio of summer-to-annual rainfall exceeding 55 %. The defined GMA (Fig. 2 in Liu et al. 2009) is almost identical to that shown in Fig. 2.1. The GMA presented in Wang et al. (2011) was based on alternative criteria—AR (JJA and DJF difference) exceeding 2 mm day^{-1} and 70 % of the annual mean, and it also agrees with the results shown in Fig. 2.1 and other similar studies (Wang and Ding 2008; Liu et al. 2009). Therefore, the defined GMA is not very sensitive to the two criteria with some modifications.

Total rainfall amount during a local summer (JJA for the NH, and DJF for the SH) is the major factor determining the amplitude of AR. Generally, a larger AR (wet-dry season contrast) reflects a more active monsoon. Therefore, the total GM

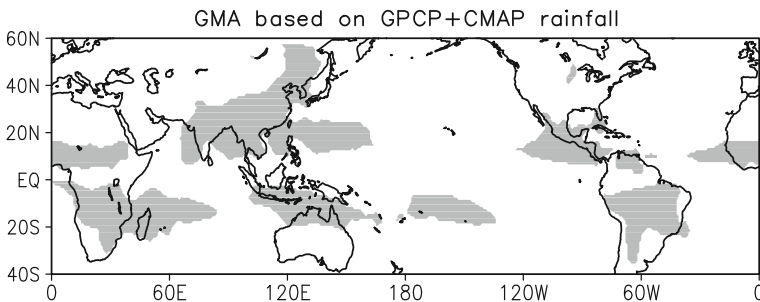


Fig. 2.1 Observed global monsoon area (*shaded area*) derived from the average of GPCP and CMAP climatological rainfall for 1979–2008

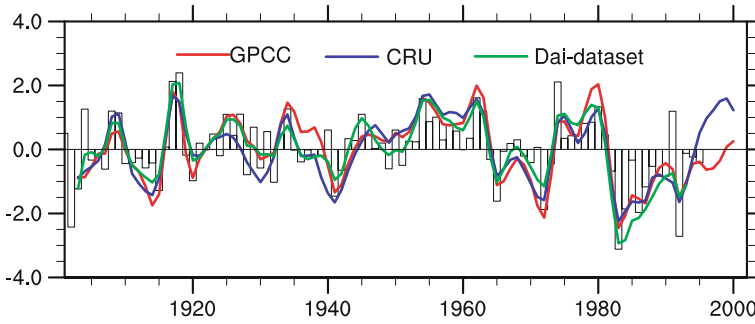


Fig. 2.2 Time series of normalized global land monsoon precipitation anomalies. The bars denote the GMP over land based on the data compiled by Dai (*Dai-dataset*). The anomalies are calculated relative to the mean of 1951–1979, using the precipitation datasets developed by the Global Precipitation Climatology Centre (*GPCC*) and by the Climate Research Unit (*CRU*), and the *Dai-dataset*. The *red*, *blue*, and *green* curves are 5-year running means of *GPCC*, *CRU* and *Dai-dataset*, respectively. According to Zhang and Zhou (2011)

precipitation (GMP)—the sum of summer rainfall within the GMA—is proposed to describe the monsoon strength (Wang and Ding 2006, 2008; Liu et al. 2009). Given that the global circulation and the land-sea surface-temperature contrast may experience significant changes from one climate condition to another, induced by sea-surface-temperature (SST) anomalies or anthropogenic forcing, the GMA may be subject to some temporal/spatial variability. To describe the GMP change associated with a varying GMA, the global monsoon intensity (GMI) index, which measures the GMP amount per unit area, was introduced (Zhou et al. 2008a; Hsu et al. 2011; Wang et al. 2011). Because the area in each grid box varies with latitude, an area-conserving metric is applied when calculating the GMA and GMP. The long-term variability of GMA, GMP, and GMI over the past decades and their projected changes under certain global warming scenarios, are reviewed in the following two sections, respectively.

2.3 Observed Changes in Global Monsoon Activity

2.3.1 Trends in GM Precipitation in the Twentieth Century

After the concept of the GM was proposed, a number of researchers began to investigate the variability of GMP over continental monsoon areas inhabited by billions of people. Chase et al. (2003) analyzed the variation of land precipitation along with surface pressure and upper-level divergence in the Asian, Australian, and African monsoon regions between 1950 and 1998. Consistent reductions in land rainfall and monsoonal circulations have been detected over the monsoon

regions globally since 1950. However, this decreasing trend has leveled off since 1979, when the strongest global warming has been reported in terms of averaged surface temperature. Using four sets of rain gauge observations for the 1948–2003 period, Wang and Ding (2006) also pointed out an overall downward trend in rainfall over land within global monsoon domains, particularly before 1980. The weakening of GMP over land was mainly attributed to the decreased summer monsoon rainfall in the NH because the monsoon rainfall in the SH showed no significant trend over the same period (Wang and Ding 2006). Zhou et al. (2008a) further pointed out that not only the monsoon precipitation intensity, but also the total monsoon area, contributed to this weakening trend in global land monsoon rainfall from 1949 to 2002.

Using a century-long observational rainfall dataset, Zhang and Zhou (2011) found that the global land monsoon precipitation exhibited a significant multi-decadal variability during the twentieth century (Fig. 2.2). A significant upward trend in the global land monsoon precipitation was shown in the first half of the century (1901–1955), followed by a downward trend in the latter half (1955–2001), as documented in other studies (Chase et al. 2003; Wang and Ding 2006; Zhou et al. 2008a). Because of this multi-decadal change, the overall trend for the twentieth century (1901–2001) was not statistically significant at the 95 % confidence level.

As discussed above, the results based on rain-gauge observations show no significant trend in rainfall over the global land monsoon areas since 1979. Was this the same for the precipitation change over the oceanic monsoon regions? Wang and Ding (2006) used the GPCP dataset to examine the GMP over oceans and found a significant increasing trend from 1979 to 2003. This change in oceanic monsoon rainfall, however, is not robust and depends on data sources (Zhou et al. 2008b; Hsu et al. 2011). In contrast to the GPCP data, the CMAP data indicate a weak declining monsoon rainfall over the global oceanic monsoon regions for the period of 1979–2008. The inconsistency of rainfall variability over the oceans between the GPCP and CMAP datasets was attributed to different algorithms used to retrieve the precipitation from the satellite data (Gruber et al. 2000).

The trends in global oceanic monsoon rainfall have dominated the trends in total GMP over the past three decades (Wang and Ding 2006; Zhou et al. 2008b; Hsu et al. 2011). The GMP showed an increasing trend from 1979 to 2008 based on the GPCP rainfall data, while it revealed a downward tendency over the same period using the CMAP dataset (Fig. 2.3). Zhou et al. (2008b) found that the oceanic monsoon rainfall derived from the GPCP dataset was highly correlated with that of the Special Sensor Microwave Imager (SSM/I), which might be the best available precipitation estimates over the ocean. This suggests that the trend in GMP obtained from the GPCP data is probably more reliable than that from the CMAP data. With a focus on the monsoon change at the hemispheric scale, Wang et al. (2013) found consistent enhancements of NH monsoon rainfall and of the Walker and Hadley circulations from 1979 to 2011.

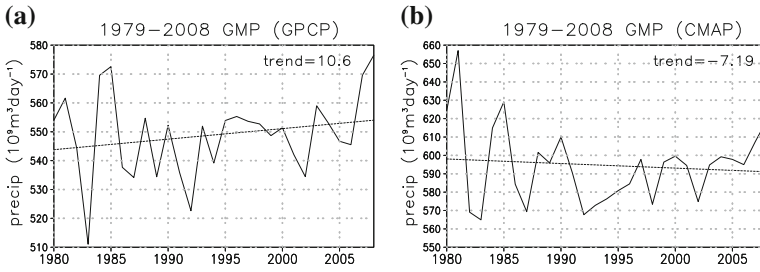


Fig. 2.3 **a** Time series of global monsoon precipitation (GMP; units: $10^9 \text{ m}^3 \text{ day}^{-1}$) calculated from (s) the GPCP and **b** the CMAP datasets for 1979–2008. The linear trend of each time series is indicated by a *dotted line*, with the linear trend [units: $10^9 \text{ m}^3 \text{ day}^{-1} (29 \text{ year})^{-1}$] noted on each panel. (Adapted from Hsu et al. 2011)

2.3.2 Factors Controlling the GMP Change

Variations in GMP can be attributed to tropical atmospheric responses to varying forcing fields, such as SST, shortwave forcing resulting from the effect of aerosols, and longwave forcing induced by growing greenhouse gas emissions. Wang et al. (2012) discussed the mechanisms regulating the NH summer monsoon rainfall over land and adjacent ocean areas. They suggested that the zonal contrast of eastern and western Pacific SST plays an important role in causing the enhanced NH monsoon precipitation. The recent trend of eastern Pacific cooling and western Pacific warming favors the high (low) pressure anomaly in the eastern (western) Pacific and the trades that transport moisture into the Asian and African monsoon regions (Wang et al. 2013). Moreover, the intensification of NH monsoon rainfall is consistent with the increased inter-hemispheric thermal contrast. The pattern associated with a warmer NH and a cooler SH over the past three decades would induce strengthened cross-equatorial flows driven by meridional pressure gradients. As a result, more moisture is transported from the SH into the NH, favoring the monsoon rainfall in the NH (Wang et al. 2012).

Long-term simulations under different forcing fields may help to clarify the factors controlling the observed GMP changes. Zhou et al. (2008b) showed that the observed weakening trend in global land monsoon precipitation over the second half of the twentieth century was successfully reproduced by the NCAR Community Atmosphere Model version 2 (CAM2) driven by observed SSTs between 1950 and 2000. The results indicated that the changes in GMP over land may have arisen from oceanic forcing. In the second half of the twentieth century (1950–2000), significant warming trends were observed over the central-eastern Pacific Ocean and the tropical Indian Ocean. Zhou et al. (2008b) further argued that the recent warming over the central-eastern Pacific Ocean and the tropical Indian Ocean contributed to the reduction of global land monsoon precipitation during the period of 1950–2000 reported by Wang and Ding (2006).

In addition to the SST influence, aerosols have been reported to have significant impacts on regional rainfall in several ways (e.g., Turner and Annamalai 2012).

Focusing on the effect of volcanic aerosols, Kim et al. (2008) analyzed the GMP changes in the twentieth-century simulations for the period of 1951–1999 from the models participating in the third phase of the Coupled Model Intercomparison Project (CMIP3). They found that among 21 CMIP3 models, those with volcanic aerosols simulated the decreasing trends of NH land monsoon rainfall since 1950, suggesting that the natural volcanic forcing could be an important contributor to the reduction of global land monsoon precipitation. The results of Kim et al. (2008) were similar to the findings of Lambert et al. (2004), who argued that variation in land precipitation was controlled more by the natural shortwave forcing of volcanic aerosols than by the longwave forcing of greenhouse gases. External forcing associated with volcanic aerosols plays a crucial role in multi-decadal variability of torrential precipitation in both observations and model simulations (Broccoli et al. 2003; Gillett et al. 2004).

2.4 Future Projections of Global Monsoon

The rise in the average temperature of the Earth’s atmosphere and oceans—namely, global warming—has been observed since the late twentieth century and is projected with very high probability to continue in the coming century (e.g., IPCC 2007, 2013). Estimates of GM change under a warmer future climate primarily rely on projections from climate models. Thanks to great advances in computing power and numerical model developments, state-of-the-art atmospheric general circulation models (AGCMs) and ocean-atmosphere, coupled general circulation models (CGCMs) driven by various global-warming forcings, may help to provide consistent projected signals and enhance our confidence in these future GM changes. A number of robust signals related to GM change were identified from the recent modeling studies based on various multi-model ensemble (MME) approaches (Hsu et al. 2012, 2013; Chen and Sun 2013; Kitoh et al. 2013; Lee and Wang 2014). In this section, future changes in GM domain, total amount of monsoon precipitation, extreme monsoon precipitation events, timing of monsoon onset and retreat, and inter-annual variability of GM are reviewed and discussed.

2.4.1 *Changes in GM Domain*

Based on simulations of three high-resolution (20–50 km) AGCMs forced by various future SST warming patterns during the twenty-first century, Hsu et al. (2012) indicated a consistent increase of GMA under global warming. The GMA increased around 7–9 % from the end of the twentieth century to the end of the twenty-first century in these simulations. Marked expansions occurred over the oceans, which accounted for 80–90 % of the total contribution to the GMA change in these simulations.

The expansions of GM domain were also projected in the MMEs of CMIP3 and CMIP5 models, although the spread of individual models is large (Hsu et al. 2012, 2013; Kitoh et al. 2013; Lee and Wang 2014). As shown in Fig. 2.4, the GMA projections show a 3–6 % increase from the late twentieth century (1979–2003) to the end of the twenty-first century (2075–2099) based on many ensemble members (~ 20 or more) of CMIP5 models under the Representative Concentration Pathways 4.5 (RCP4.5) scenario and of CMIP3 models under the Special Report on Emissions Scenarios (SRES) A1B scenario (Chen and Sun 2013; Hsu et al. 2013; Kitoh et al. 2013). The averaged expansion of GMA was larger ($\sim 9\%$) when the models were forced with the higher greenhouse gas emissions under the RCP8.5 scenario (Kitoh et al. 2013). Even so, Hsu et al. (2013) indicated that the expansion rate of GMA is not significantly correlated with the increase in global mean surface air temperature.

Rather than analyzing MMEs based on all CMIP3 or all CMIP5 models, Lee and Wang (2014) conducted an MME analysis based on the four models among 20 CMIP5 models that most accurately simulated monsoon precipitation characteristics during the period of 1980–2005. Similar to the results of all models' MME, the four best models' MME (B4MME) projects an increased GMA with a change rate of 4.6 % (2.6 % for land and 6.3 % for ocean) from the end of the twentieth century (1980–2005) to the end of the twenty-first century (2070–2095) under the RCP4.5 scenario. However, this change does not exceed the uncertainty measured by a standard deviation of inter-model spread.

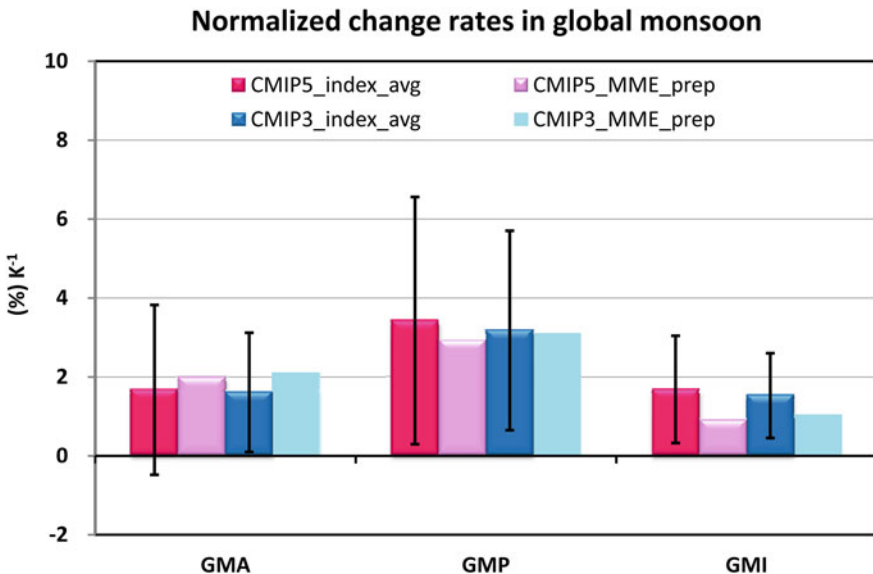


Fig. 2.4 Averages and inter-model standard deviations [red (blue) bars with whiskers] of GMA, GMP and GMI change rates between RCP4.5 (A1B) from 2075 until 2099, and historical (20C3 M) from 1979 to 2003 in 19 CMIP5 (24 CMIP3) simulations. Pink (light blue) bars show the change rates calculated from the CMIP5 (CMIP3) multi-model ensemble mean precipitation. (Adapted from Hsu et al. 2013)

According to the CMIP5 MME results, under the RCP4.5, the increased GMA will be distributed along the edges of the present-day GMA, especially for the global oceanic monsoon regions (Hsu et al. 2013). This is consistent with the B4MME results of Lee and Wang (2014), which suggested that the monsoon domain will tend to increase over oceanic monsoon regions while it will apparently not change over land except for a westward movement of Asian continental monsoon areas. Based on the RCP8.5 simulations, Kitoh et al. (2013) identified GMA expansions mainly over the central-to-eastern tropical Pacific, the southern Indian Ocean, and eastern Asia.

The future expansion of GMA may be attributed to both an increased annual range of precipitation under global warming (Chou and Lan 2012) and a stronger summer-to-annual rainfall ratio (Hsu et al. 2012; Lee and Wang 2014). Hsu et al. (2013) analyzed the absolute change of monthly rainfall within the GMA and found a prominent increase in local summer monsoon rainfall over the globe. Projected winter rainfall within the GMA, however, shows less significant change, with a small increase (decrease) in the NH (SH). These results indicate that global warming may induce a wetter summer over the GM regions, and enhance the contrast between rainy and dry seasons (especially in the SH).

2.4.2 Changes in GM Precipitation and Intensity

The expansion of the GMA may cause changes in GMP, as a larger monsoon domain would receive more rainfall. As shown in Fig. 2.4, the MME indicates a 6–9 % increase in GMP under the SRES A1B and RCP4.5 scenarios (Hsu et al. 2013), and much more (~16.6 %) in the RCP8.5 scenarios from the end of the twentieth century to the end of the twenty-first century (Kitoh et al. 2013). Due to a greater rate of increase of GMP than of GMA, the GM intensity, which is defined as the monsoon precipitation amount per unit area, will tend to strengthen in future warmer climate. The increase of GMI from the end of the twentieth century until the end of the twenty-first century ranges from 2 to 4 % in the CMIP3 and CMIP5 MME results, respectively (Fig. 2.4).

Precipitation extremes occurring in all regional monsoons are projected to increase at a much greater rate than the GMP (Kitoh et al. 2013). For example, GMP will increase by –6.5 to 12.9 % by the end of the twenty-first century, according to the RCP8.5 simulations, while the simple daily precipitation intensity index, defined as total precipitation divided by the number of rainy days (≥ 1 mm), shows –0.7 to 14.7 % increase. The index of seasonal maximum precipitation total over five consecutive days within the global monsoon areas shows an even greater increase (6.2–22.1 %) under the RCP8.5 scenario. As well as the increase in extreme precipitation events, indices of extreme dry events (such as maximum number of consecutive no-rain days) within the GMA are projected to increase (Lu and Fu 2010; Turner and Annamalai 2012). This suggests that although the frequency of precipitation events would decrease in a future warmer climate, the precipitation intensity of individual events could be greater (Kitoh et al. 2013).

Lee and Wang (2014) illustrated the spatial distribution of GMP change based on the B4MME (Fig. 2.5). The CMIP5 models projected a remarkable enhancement (reduction) of monsoon rainfall over Asia (northern America). Monsoon rainfall over Australia and Africa also show positive contributions to the increased GMP, but with less significance and robustness. The relative contributions from regional monsoons to the GMP projected by the B4MME generally agree with those derived from the CMIP5 models' MME (Kitoh et al. 2013); in other words, the Eastern-hemisphere monsoons will produce more precipitation than the Western-hemisphere monsoons, and the NH monsoons will produce more precipitation than the SH monsoons. This means that future changes in GMP can be characterized by a prominent east–west contrast and a north–south asymmetry. As with the summer mean monsoon rainfall projections, the extreme precipitation events are also projected to increase most significantly in the Asian monsoon domain, suggesting that the Asian monsoon is particularly sensitive to global warming (Kitoh et al. 2013).

To better understand the physical processes that cause the increase in GMP projected by the CMIP5 models, Hsu et al. (2013) examined a column-integrated moisture budget within the GMA in present-day and future-climate simulations, respectively.

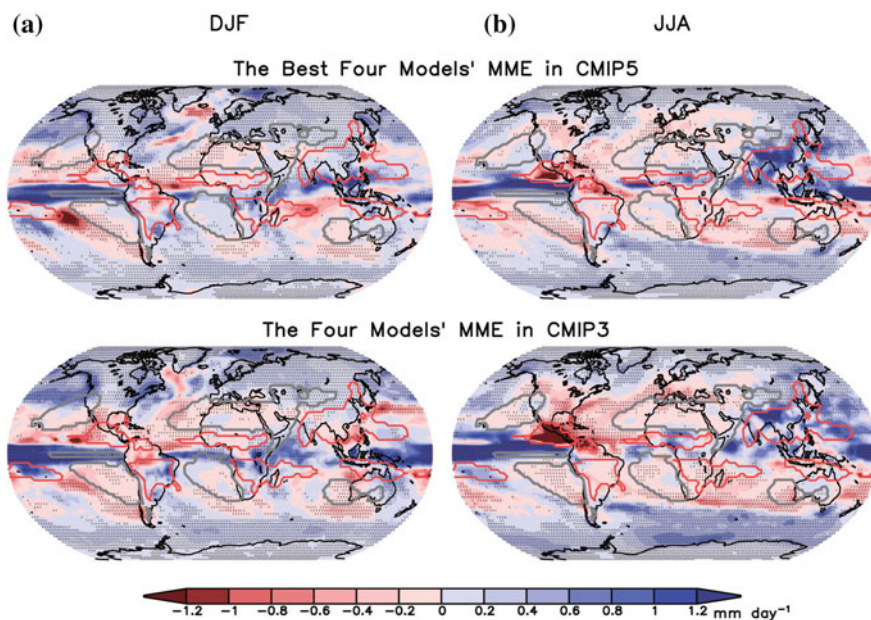


Fig. 2.5 Changes in **a** annual mean precipitation, and **b** annual range of precipitation. The annual range is defined as absolute value of JJAS mean minus DJFM mean precipitation rate. Changes are given for the RCP4.5 (A1B) simulation for 2070–2095 relative to the historical simulation for 1980–2005, in CMIP5 (CMIP3) in the *upper (bottom)* panels. Red contours delineate the GMA. (Adapted from Lee and Wang 2014)

The column-integrated moisture tendency equation is

$$\frac{\partial w}{\partial t} + \langle \nabla \cdot (q\mathbf{V}) \rangle = E - P \quad (2.1)$$

where w is precipitable water (total column water vapor), t is time, $\langle \rangle$ indicates a vertical integration from 1,000 to 100 hPa, ∇ is the horizontal gradient operator, q is specific humidity, \mathbf{V} is the horizontal vector wind, E is evaporation, and P is precipitation. This equation assumes that the condensates immediately fall to the surface as precipitation after they form. Although w and q differ between the present-day state and the future-climate state, they are assumed to be in a state of equilibrium in both periods. Thus, for each period, the tendency term ($\partial w/\partial t$) vanishes. The diagnostic equation of GMP change is then derived based on the difference of the remaining terms between the present-day and future-climate states. The change in GMP may be attributed to changes in horizontal moisture advection, moisture convergence associated with mass convergence (or vertical motion), and surface evaporation, as shown in the following equation:

$$\Delta \text{GMP} = -\Delta \langle V \cdot \nabla q \rangle - \Delta \langle q \nabla \cdot V \rangle + \Delta E. \quad (2.2)$$

The operator Δ represents the difference between future-climate and present-day simulations (future minus present-day).

The diagnostic results of CMIP5 models show that increases in both moisture convergence and surface evaporation will contribute to increased GMP, whereas moisture advection will contribute insignificantly to GMP change (Fig. 2.6a). Because the changes in atmospheric moisture and circulation affect both moisture convergence and surface evaporation, it is necessary to examine their relative contributions. The changes in moisture convergence and surface evaporation may be decomposed into three terms, as shown below:

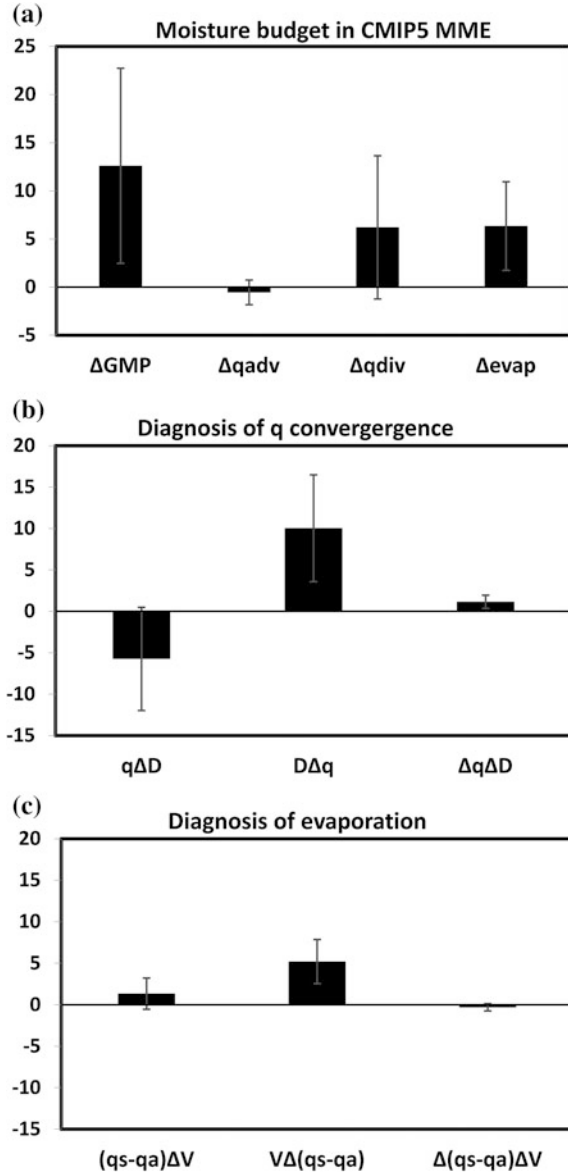
$$-\Delta \langle q \times D \rangle = -\langle q_{\text{pd}} \times \Delta D \rangle - \langle \Delta q \times D_{\text{pd}} \rangle - \langle \Delta q \times \Delta D \rangle, \quad (2.3)$$

$$\begin{aligned} \Delta E &= \Delta[\alpha |\mathbf{V}|(q_s - q_a)] \\ &= \alpha[\Delta |\mathbf{V}| \times (q_s - q_a)_{\text{pd}} + |\mathbf{V}|_{\text{pd}} \times \Delta(q_s - q_a) + \Delta |\mathbf{V}| \times \Delta(q_s - q_a)], \end{aligned} \quad (2.4)$$

where D denotes divergence, $\alpha = L\rho C_E$, L is latent heat, ρ is the air density at sea level, C_E is the exchange coefficient, $|\mathbf{V}|$ is surface wind speed, q_s and q_a are the specific humidity at sea surface and at 10 m, respectively, and the subscript ‘pd’ denotes the present-day simulation. The first term on the right-hand sides of Eqs. (2.3) and (2.4) is associated with circulation change, which may be regarded as a dynamic contributor. The second term involves the change of water-vapor content; thus, it reflects the thermodynamic effect on the GMP. The third term is a nonlinear term including the effects of both moisture and circulation changes.

A robust feature simulated by the CMIP5 models is that the thermodynamic effect due to increased water-vapor content plays an important role in enhancing

Fig. 2.6 a Moisture processes responsible for the GMP change based on 19 CMIP5 MME. *Left to right* changes in GMP, horizontal moisture advection, moisture convergence, and surface evaporation within the GMA (Units: 10^{14} W). Whiskers indicate inter-model standard deviations of the 19 models **b** and **c** are the same as **(a)**, except for the diagnoses of moisture convergence change and evaporation change, respectively. *Left to right* contributions of dynamic effect associated with circulation change, thermodynamic component associated with water vapor change, and the nonlinear product of the two changes. (Adapted from Hsu et al. 2013)



both moisture convergence (Fig. 2.6b) and evaporation (Fig. 2.6c). However, the dynamic effect is less robust and shows different contributions to moisture convergence and evaporation between different models. The CMIP5 models suggest that a weaker monsoon convergence flow under global warming will have a tendency to decrease monsoon rainfall (Fig. 2.6b). Although this dynamic component offsets the thermodynamic component to a large extent, the thermodynamic

component still dominates the increased GMP (Fig. 2.6a). As for evaporation, the dynamic effect related to the increased surface wind speed reveals positive, but minor, contributions to GMP in the averaged result of CMIP5 models (Fig. 2.6c). These diagnostic results from Hsu et al. (2013) confirm the findings in Cherchi et al. (2011), Hsu et al. (2012), and Kitoh et al. (2013), which emphasized the role of enhanced moisture convergence and evaporation in the increase of GMP.

2.4.3 Changes in Monsoon Onset and Retreat

Aside from the total amount of monsoon precipitation (GMP), the temporal distribution of rainfall throughout the rainy season is another important issue. Changes in the timing of monsoon onset and retreat, and the durations of monsoon rainy periods, will strongly affect agricultural and socio-economic policies. The onset (retreat) of the monsoon rainy season is generally concurrent with an abrupt increase (decrease) in precipitation. Wang and LinHo (2002) defined the timing of monsoon onset (retreat) as the date when the relative climatological mean precipitation (i.e., the difference between the climatological daily precipitation and dry month) first exceeds (drops below) 5 mm day^{-1} . Using this definition, Kitoh et al. (2013) examined the changes in monsoon onset and retreat in each land monsoon domain around the globe. The CMIP5 models project significant changes in the timing of monsoon onset and retreat over land in Asia and Australia. The onset date of the Asian-Australian monsoon tends to advance, while the monsoon retreat is delayed, indicating a lengthening of the monsoon rainy season. Similar projected results were identified from the B4MME of CMIP5 models (Lee and Wang 2014) and from the CMIP3 models (Kumar et al. 2011). The CMIP5 MME projections of monsoon onset and retreat changes in the American and African monsoon regions were less significant and had a larger spread (Kitoh et al. 2013).

2.4.4 Changes in Inter-annual Variability of GMP

The El Niño/Southern Oscillation (ENSO) has been a crucial factor in modulating the year-to-year GMP variations in recent decades (e.g., Zhou et al. 2008b; Wang et al. 2012). According to the observations, the GMP has experienced a great inter-annual variation and has been significantly negatively correlated with the central-eastern Pacific SST averaged over the monsoon year defined from May to the following April (Yasunari 1991). The negative correlation coefficient between the ENSO and GMP was found consistently in the CMIP5 pre-industry control simulations (Hsu et al. 2013), confirming that the inter-annual variability of the GMP was largely due to internal processes of the atmosphere (Wang et al. 2012).

The change in ENSO amplitude in a warmer climate shows a large diversity among the CMIP5 model projections. In terms of the Niño 3 or Niño 3.4 index in

future simulations, some models projected increasing ENSO variability, some showed less variability, and some exhibited no change (Guilyardi et al. 2012; Kim and Yu 2012; Stevenson et al. 2012). The mean of CMIP5 projections indicates a stable or slightly weaker ENSO in the RCP4.5 simulations relative to the present-day simulations (Kim and Yu 2012; Hsu et al. 2013). Although the change in ENSO intensity is uncertain in these future projections, the general ENSO-GMP relationship remains significant and even becomes stronger under global warming. Hsu et al. (2013) found that the negative correlation coefficient between the Niño 3.4 index and GMP may increase from the present day to the end of the twenty-first century. Moreover, the year-to-year standard deviation of GMP is intensified in the RCP 4.5 simulations. This suggests that more extreme monsoon years might occur in the future (Turner and Annamalai 2012). A large portion of the change in the year-to-year GMP comes from the land monsoon rather than the oceanic monsoon (Hsu et al. 2013).

2.5 Conclusions

Monsoon is a response of the climate system to the annual variation in solar forcing. It is characterized by seasonal wind reversals and a wet-dry season contrast (Ramage 1971; Webster et al. 1987). From a global perspective, the annual variation of insolation is the essential driver for all of the regional monsoons around the world, although different land-sea configurations control the variability of individual monsoon systems. Thus, the monsoon rainfall features over the globe can be viewed as parts of an integrated GM system, which is associated with a persistent global-scale overturning of the atmosphere, varying with the time of year (Trenberth et al. 2000, 2006).

The GM precipitation has profound impacts on billions of people living in the GM regions. Its variability and possible changes in future warmer climates have attracted growing interest in recent years. Wang and Ding (2006) used the characteristics of monsoon precipitation to delineate the GMA, which includes the annual range of rainfall exceeding 2 mm day^{-1} and the ratio of summer-to-annual rainfall being larger than 35 %. The GMP is then defined as the local summer rainfall within the GMA, and the GMI measures the total GMP amount per unit area (Zhou et al. 2008a; Hsu et al. 2011). Similar definitions of GM indices using different months or different rainfall ratios have been proposed, but the resultant GMA and the change in GM intensity are not sensitive to the fine details of these criteria (Liu et al. 2009; Hsu et al. 2011; Wang et al. 2012).

The long-term variation of GMP over land has been analyzed based on various rain-gauge observations (Wang and Ding 2006; Zhang and Zhou 2011). A significant phase transition of global land monsoon precipitation was identified around the 1950s. The GMP over land showed an overall increasing trend from the beginning of the twentieth century to the 1950s (Zhang and Zhou 2011); it then experienced a downward trend from 1950 to 1980, followed by an insignificant

trend until the present (Wang and Ding 2006). Because the decreasing trend of GMP over land was well reproduced by an AGCM driven by observed SSTs over the past five decades, Zhou et al. (2008b) suggested that the variability of global land monsoon rainfall would arise mainly from oceanic forcing. Besides the SST effect, the external forcing from volcanic aerosols also played an important role in the reduction of global land monsoon precipitation. The CMIP3 models with volcanic aerosols simulated a more robust and significant downward trend in land GMP than those without volcanic aerosols (Kim et al. 2008).

Although no significant change in land GMP has been detected from the rain-gauge data since 1979 (Chase et al. 2003; Wang and Ding 2006), an increasing trend in the overall GMP (sum of land and oceanic monsoon rainfall) over the past three decades is shown in the GPCP global rainfall dataset. This increased GMP results primarily from the upward trend in global oceanic monsoon precipitation (Wang et al. 2012). In contrast to the GPCP result, a decreased GMP over the ocean is shown in the CMAP global rainfall dataset (Hsu et al. 2011), reflecting the uncertainty of global oceanic monsoon rainfall among different precipitation datasets (Zhou et al. 2008b; Hsu et al. 2011). Wang et al. (2013) calculated the trends in the GMP using the average of the GPCP and CMAP rainfall datasets, along with the variation of tropical circulations to assess the NH monsoon change. Their results indicated that all the summer monsoon rainfall in the NH, as well as the Hadley and Walker circulations, have been enhanced since 1979. This intensification of NH monsoon activity is related to the recent trend of SST cooling in the eastern Pacific and warming in the western Pacific (Wang et al. 2013), enhancing the trades that transport moisture into the Asian and African monsoon regions.

By the end of the twenty-first century, the GMP is projected to increase by 6–9 % (~ 16 %) relative to the end of the twentieth century, based on the CMIP5 RCP4.5 (8.5) simulations (Kitoh et al. 2013; Hsu et al. 2013). The enhanced GMP can be attributed to the expansion of GMA and the enhancement of GMI. The findings of overall increases in the GM area, precipitation, and intensity in the CMIP5 projections, are consistent with the CMIP3 model projections (Hsu et al. 2013), although some differences of regional monsoon characteristics have been found between the two generations of CMIP models (Lee and Wang 2014). On the regional scale, a large spread of GM variability was detected among model projections, indicating much more uncertainty in the projected regional monsoon changes (Giorgi et al. 2001; Kitoh et al. 2005; Cook and Vizy 2006; Li et al. 2006; Lu and Fu 2010; Hsu and Li 2012; Moise et al. 2012; Turner and Annamalai 2012; Sperber et al. 2013).

Future projections of increased GMP are mainly based on changes to the hydrological cycle, induced by warmer temperatures. An examination of column-integrated moisture budget in the GMA suggests that increases in moisture convergence and surface evaporation are both responsible for increases in GMP, while the effect of moisture advection is insignificant (Hsu et al. 2012, 2013; Kitoh et al. 2013). Further analysis has indicated that the thermodynamic effect associated with increased water vapor contributes positively to moisture convergence, but this

contribution is partly offset by the dynamic effect related to the weakening of the monsoon overturning (divergent) circulation. This partial cancellation between the thermodynamic and dynamic components of moisture convergence was also found in the modulation of regional monsoon precipitation (Cherchi et al. 2011; Moise et al. 2012). Regarding the future enhancement of evaporation within the GMA, moisture analysis suggests that the increase in specific humidity over the ocean due to increasing SSTs will play a major role. However, the future change related to surface wind speed shows different results between the high-resolution AGCMs (Hsu et al. 2012) and CMIP5 models (Hsu et al. 2013).

In summary, from the global perspective, the GM system is likely to show enhanced activity in a warmer climate. The increased area, precipitation, and intensity of the future GM are consistently projected by GCMs with different physics and various forcing scenarios. However, the models also show discrepancies in terms of individual monsoon regions, which reduce our confidence in future regional monsoon changes (IPCC 2007, 2013). Unlike the GM change that is largely controlled by planetary-scale forcings, effects on regional monsoon variation are much more complicated (IPCC 2007; Turner and Annamalai 2012). How individual monsoons may respond to a warming climate will be discussed in the following chapters.

Acknowledgments This work was supported by the NSFC grant (41375100), Research Project of the Chinese Ministry of Education (213014A), Natural Science Foundation of Jiangsu Province, China (BK20140046), and by the International Pacific Research Center (IPRC) at University of Hawaii.

References

- Adler RF et al (2003) The version 2 global precipitation climatology project (gpcp) monthly precipitation analysis (1979–present). *J Hydrometeorol* 4:1147–1167. doi:[10.1175/1525-7541\(2003\)004<1147:TVGPCP>2.0.CO;2](https://doi.org/10.1175/1525-7541(2003)004<1147:TVGPCP>2.0.CO;2)
- Broccoli AJ, Dixon KW, Delworth TL, Knutson TR, Stouffer RJ, Zeng F (2003) Twentieth-century temperature and precipitation trends in ensemble climate simulations including natural and anthropogenic forcing. *J Geophys Res* 108:4798. doi:[10.1029/2003JD003812](https://doi.org/10.1029/2003JD003812)
- Chase TN, Knaff JA, Pielke RA Sr, Kalnay E (2003) Changes in global monsoon circulations since 1950. *Nat Hazards* 29:229–254
- Chen H-P, Sun J-Q (2013) How large precipitation changes over global monsoon regions by CMIP5 models? *Atmos Oceanic Sci Lett* 6:306–311. doi:[10.3878/j.issn.1674-2834.13.0002](https://doi.org/10.3878/j.issn.1674-2834.13.0002)
- Cherchi A, Alessandri A, Masina S, Navarra A (2011) Effects of increased CO₂ levels on monsoons. *Clim Dyn* 37:83–101. doi:[10.1007/s00382-010-0801-7](https://doi.org/10.1007/s00382-010-0801-7)
- Chou C, Lan C-W (2012) Changes in the annual range of precipitation under global warming. *J. Climate* 25:222–235. doi:[10.1175/JCLID-11-00097.1](https://doi.org/10.1175/JCLID-11-00097.1)
- Cook KH, Vizy EK (2006) Coupled model simulations of the West African monsoon system: twentieth- and twenty-first-century simulations. *J Climate* 19:3681–3703. doi:[10.1175/JCLI3814.1](https://doi.org/10.1175/JCLI3814.1)
- Davidson N, McBride J, McAvaney B (1983) The onset of the Australian monsoon during winter MONEX: synoptic aspects. *Mon Wea Rev* 111:496–516

- Ding YH (1994) Monsoons over China. Springer, Heidelberg, p 419
- Gillett NP, Weaver AJ, Zwiers FW, Wehner MF (2004) Detection of volcanic influence on global precipitation. *Geophys Res Lett* 31:L12217. doi:[10.1029/2004GL020044](https://doi.org/10.1029/2004GL020044)
- Giorgi F, Whetton PH, Jones RG, Christensen JH, Mearns LO, Hewitson B, vonStorch H, Francisco R, Jack C (2001) Emerging patterns of simulated regional climatic changes for the 21st century due to anthropogenic forcings. *Geophys Res Lett* 28:3317–3320. doi:[10.1029/2001GL013150](https://doi.org/10.1029/2001GL013150)
- Goswami BN (2005) The Asian monsoon: interdecadal variability. In: Wang B (ed) *The Asian monsoon*. Praxis, Springer, Berlin Heidelberg, pp 295–327
- Guilyardi E, Bellenger H, Collins M, Ferrett S, Cai W, Wittenberg A (2012) A first look at ENSO in CMIP5. *CLIVAR Exchanges* 58:29–32
- Gruber A, Su X, Kanamitsu M, Schemm J (2000) The comparison of two merged rain gauge-satellite precipitation datasets. *Bull Amer Meteor Soc* 81:2631–2644
- Higgins RW, Yao Y, Wang XL (1997) Influence of the North American monsoon system on the U.S. summer precipitation regime. *J Climate* 10:2600–2622
- Hsu P, Li T, Wang B (2011) Trends in global monsoon area and precipitation over the past 30 years. *Geophys Res Lett* 38:L08701. doi:[10.1029/2011GL046893](https://doi.org/10.1029/2011GL046893)
- Hsu P, Li T (2012) Is “rich-get-richer” valid for Indian Ocean and Atlantic ITCZ? *Geophys Res Lett* 39:L13705. doi:[10.1029/2012GL052399](https://doi.org/10.1029/2012GL052399)
- Hsu P, Li T, Luo J-J, Murakami H, Kitoh A, Zhao M (2012) Increase of global monsoon area and precipitation under global warming: a robust signal? *Geophys Res Lett* 39:L06701. doi:[10.1029/2012GL051037](https://doi.org/10.1029/2012GL051037)
- Hsu P-C, Li T, Murakami H, Kitoh A (2013) Future change of the global monsoon revealed from 19 CMIP5 models. *J Geophys Res Atmos* 118:1247–1260. doi:[10.1002/jgrd.50145](https://doi.org/10.1002/jgrd.50145)
- Intergovernmental Panel on Climate Change (IPCC) (2007) *Climate change 2007*. In: Solomon S et al (eds) *The physical science basis*. Contribution of working group I to the fourth assessment report of the IPCC. Cambridge University Press, Cambridge, UK
- IPCC (2013) *Climate change 2013: the physical science basis*. In: Contribution of working group I to the fifth assessment report of the IPCC, intergovernmental panel on climate change, Geneva, Switzerland
- Kim H-J, Wang B, Ding Q (2008) The global monsoon variability simulated by CMIP3 coupled climate models. *J Clim* 21:5271–5294
- Kim ST, Yu J-Y (2012) The two types of ENSO in CMIP5 models. *Geophys Res Lett* 39:L11704. doi:[10.1029/2012GL052006](https://doi.org/10.1029/2012GL052006)
- Kitoh A, Hosaka M, Adachi Y, Kamiguchi K (2005) Future projections of precipitation characteristics in East Asia simulated by the MRI CGCM2. *Adv Atmos Sci* 22:467–478
- Kitoh A, Endo H, Krishna Kumar K, Cavalcanti IFA, Goswami P, Zhou T (2013) Monsoons in a changing world: a regional perspective in a global context. *J Geophys Res Atmos* 118:3053–3065. doi:[10.1002/jgrd.50258](https://doi.org/10.1002/jgrd.50258)
- Kumar KK et al (2011) The once and future pulse of Indian monsoonal climate. *Clim Dyn* 36:2159–2170
- Lambert FH, Stott PA, Allen MR, Palmer MA (2004) Detection and attribution of changes in 20th century land precipitation. *Geophys Res Lett* 31:L10203. doi:[10.1029/2004GL019545](https://doi.org/10.1029/2004GL019545)
- Lee J-Y, Wang B (2014) Future change of global monsoon in the CMIP5. *Clim Dyn* 42:101–119. doi:[10.1007/s00382-012-1564-0](https://doi.org/10.1007/s00382-012-1564-0)
- Li W, Fu R, Dickinson RE (2006) Rainfall and its seasonality over the Amazon in the 21st century as assessed by the coupled models for the IPCC AR4. *J Geophys Res Atmos* 111:D02111. doi:[10.1029/2005JD006355](https://doi.org/10.1029/2005JD006355)
- Liu J, Wang B, Ding Q, Kuang X, Soon W, Zorita E (2009) Centennial variations of the global monsoon precipitation in the last millennium: Results from ECHO-G model. *Clim* 22:2356–2371. doi:[10.1175/2008JCLI2353.1](https://doi.org/10.1175/2008JCLI2353.1)
- Lu R, Fu Y (2009) Intensification of East Asian summer rainfall interannual variability in the twenty-first century simulated by 12 CMIP3 coupled models. *J Clim* 23:3316–3331. doi:[10.1175/2009JCLI3130.1](https://doi.org/10.1175/2009JCLI3130.1)

- McBride JL (1987) The Australian summer monsoon. In: Chang CP, Krishnamurti TN (eds) *Monsoon meteorology*. Oxford University Press, New York, pp 203–231
- Moise AF, Colman RA, Brown JR (2012) Behind uncertainties in projections of Australian tropical climate: analysis of 19 CMIP3 models. *J Geophys Res Atmos* 117:D10103. doi:[10.1029/2011JD017365](https://doi.org/10.1029/2011JD017365)
- Ramage CS (1971) *Monsoon meteorology*. Academic Press, London, p 296
- Sperber KR, Annamalai H, Kang I-S, Kitoh A, Moise A, Turner AG, Wang B, Zhou T (2013) The Asian summer monsoon: an intercomparison of CMIP5 vs. CMIP3 simulations of the late 20th century. *Clim Dyn* 41:2711–2744. doi:[10.1007/s00382-012-1607-6](https://doi.org/10.1007/s00382-012-1607-6)
- Stevenson S, Fox-Kemper B, Jochum M, Neale R, Deser C, Meehl G (2012) Will there be a significant change to El Niño in the 21st century? *J Clim* 25:2129–2145, cCSM4 special issue. doi:[10.1175/JCLI-D-11-00252.1](https://doi.org/10.1175/JCLI-D-11-00252.1)
- Sultan B, Janicot S (2003) The West African monsoon dynamics. Part II: the “preonset” and “Onset” of the summer monsoon. *J Clim* 16:3407–3427
- Tao S, Chen L (1987) A review of recent research on the East Asian summer monsoon in China. In: Chang C-P, Krishnamurti TN (eds) *Monsoon meteorology*, Oxford University Press, pp 60–92
- Trenberth KE, Stepaniak DP, Caron JM (2000) The global monsoon as seen through the divergent atmospheric circulation. *J Clim* 13:3969–3993
- Trenberth KE, Hurrell JW, Stepaniak DP (2006) The Asian monsoon: global perspectives. In: Wang B (ed) *The Asian monsoon*, Praxis Publishing Ltd., Chichester, 781 pp
- Turner AG, Annamalai A (2012) Climate change and the South Asian summer monsoon. *Nat Clim Change* 2 doi:[10.1038/NCLIMATE1495](https://doi.org/10.1038/NCLIMATE1495)
- Vera C et al (2006) Toward a unified view of the American monsoon systems. *J Clim* 19:4977–5000. doi:[10.1175/JCLI3896.1](https://doi.org/10.1175/JCLI3896.1)
- Wang B, Lin Ho (2002) Rainy season of the Asian-Pacific summer monsoon. *J Clim* 15:386–398
- Wang B, Ding Q (2006) Changes in global monsoon precipitation over the past 56 years. *Geophys Res Lett* 33:L06711
- Wang B, Ding Q (2008) Global monsoon: dominant mode of annual variation in the tropics. *Dyn Atmos Oceans* 44:165–183
- Wang B, Ding Q, Liu J (2011) Concept of the global monsoon. In: Chang C-P, Wang B, Lau GN-C (eds) *The global monsoon system: research and forecast*, 2nd edn. World Scientific Publication Company, 608 pp
- Wang B, Liu Y, Kim H-J, Webster PJ, Yim S-Y (2012) Recent change of the global monsoon precipitation (1979–2008). *Clim Dyn* 39:1123–1135. doi:[10.1007/s00382-011-1266-z](https://doi.org/10.1007/s00382-011-1266-z)
- Wang B, Liu J, Kim H-J, Webster PJ, Yim S-Y, Xiang B (2013) Northern hemisphere summer monsoon intensified by mega-El Niño/southern oscillation and atlantic multidecadal oscillation. *PNAS* 110:5347–5352. doi:[10.1073/pnas.1219405110](https://doi.org/10.1073/pnas.1219405110)
- Webster PJ (1987) The elementary monsoon. In: Fein JS, Stephens PL (eds) *Monsoons*. Wiley-Interscience, New York
- Webster PJ et al (1998) Monsoons: processes, predictability, and the prospects for prediction. *J Geophys Res Atmos* 103:14451–14510
- Xie PP, Arkin PA (1997) Global precipitation: a 17-year monthly analysis based on gauge observations, satellite estimates, and numerical model outputs. *Bull Am Meteorol Soc* 78:2539–2558. doi:[10.1175/1520-0477\(1997\)078<2539:GPAYMA>2.0.CO;2](https://doi.org/10.1175/1520-0477(1997)078<2539:GPAYMA>2.0.CO;2)
- Yasunari T (1991) The monsoon year—a new concept of the climatic year in the tropics. *Bull Amer Meteor Soc* 72:1331–1338. doi:[http://dx.doi.org/10.1175/1520-0477\(1991\)072<1331:TMYNCO>2.0.CO;2](http://dx.doi.org/10.1175/1520-0477(1991)072<1331:TMYNCO>2.0.CO;2)
- Zhang L, Zhou T (2011) An assessment of monsoon precipitation changes during 1901–2001. *Clim Dyn* 37:279–296
- Zhou T, Yu R, Li H, Wang B (2008a) Changes in global land monsoon area and total rainfall accumulation over the last half century. *Geophys Res Lett* 35:L16707
- Zhou T, Zhang L, Li H (2008b) Ocean forcing to changes in global monsoon precipitation over recent half-century. *J Clim* 21:3833–3852